

Supplementary Information

Elastomer for Epidermal Electronics with Adjustable Adhesion Force and Stretchability by Reverse-Micelle-Induced Process

Junhyung Kim,^{a, b} Yujin Hwang,^{a,b} Sunho Jeong,^a Su Yeon Lee,^a Youngmin Choi,^{a,b} and Sungmook Jung^a

a.Division of Advanced Materials, Korea Research Institute of Chemical Technology (KRICT), 141 Gajeongro, Daejeon 305-600, Republic of Korea.

b.Department of Chemical Convergence Materials, Korea University of Science and Technology (UST), 217 Gajeongno, Yuseong-gu, Daejeon 305-350, Korea.

*To whom correspondences should be addressed.

E-mail: youngmin@kRICT.re.kr (Y.C.), mooktank@kRICT.re.kr (S.J.)

Supplementary Figures

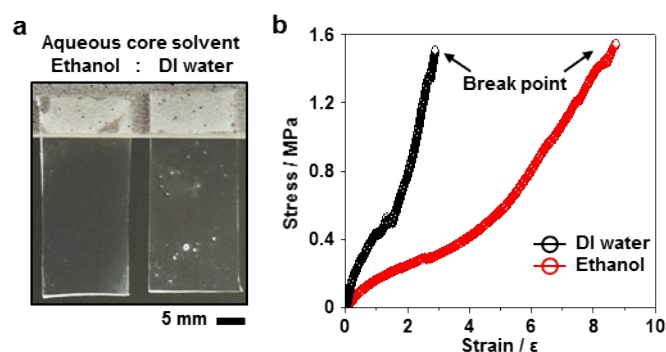


Fig. S1. Influence of aqueous core. (a) Images and (b) stress-strain curves of ethanol-based and water-based RMI films. When the aqueous core was formed of a solvent having a high boiling point, the solvent remained even after polymerization of the elastomer and it made pores.

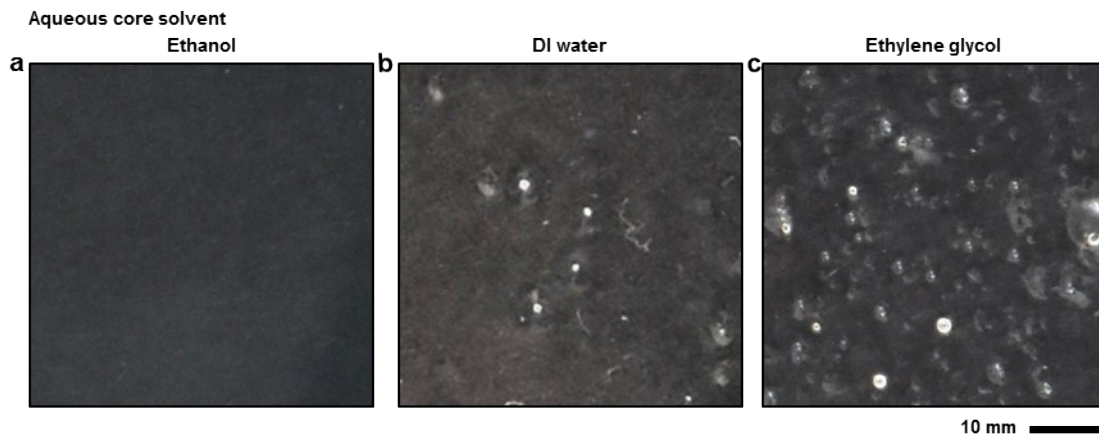


Fig. S2. Optical microscope images of RMI films made of different aqueous core solvent; (a) Ethanol, (b) DI water, and (c) Ethylene glycol.

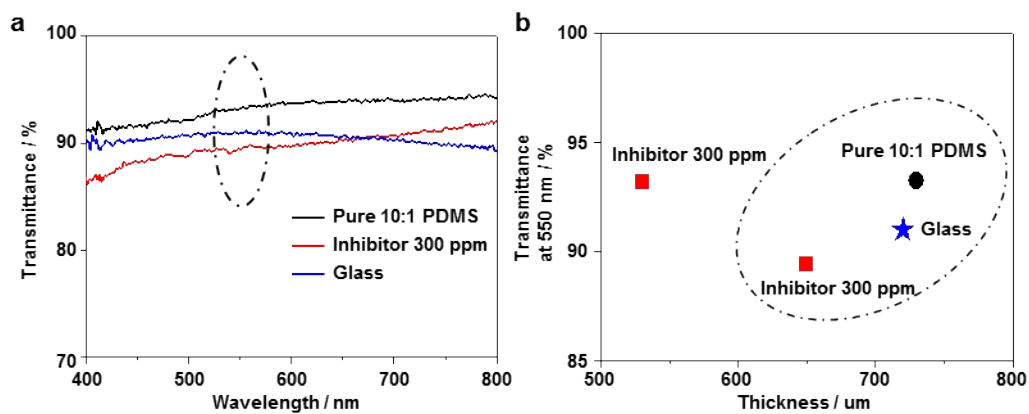


Fig. S3. Trantransparency of the RMI film. UV-Vis graph of pure 10:1 PDMS film, RMI film, and glass (10:1 PDMS-based, inhibitor: 300 ppm). (a) Transmittance scan over the full range of wavelength. (b) Transmittance change according to the thickness at 550 nm wavelength.

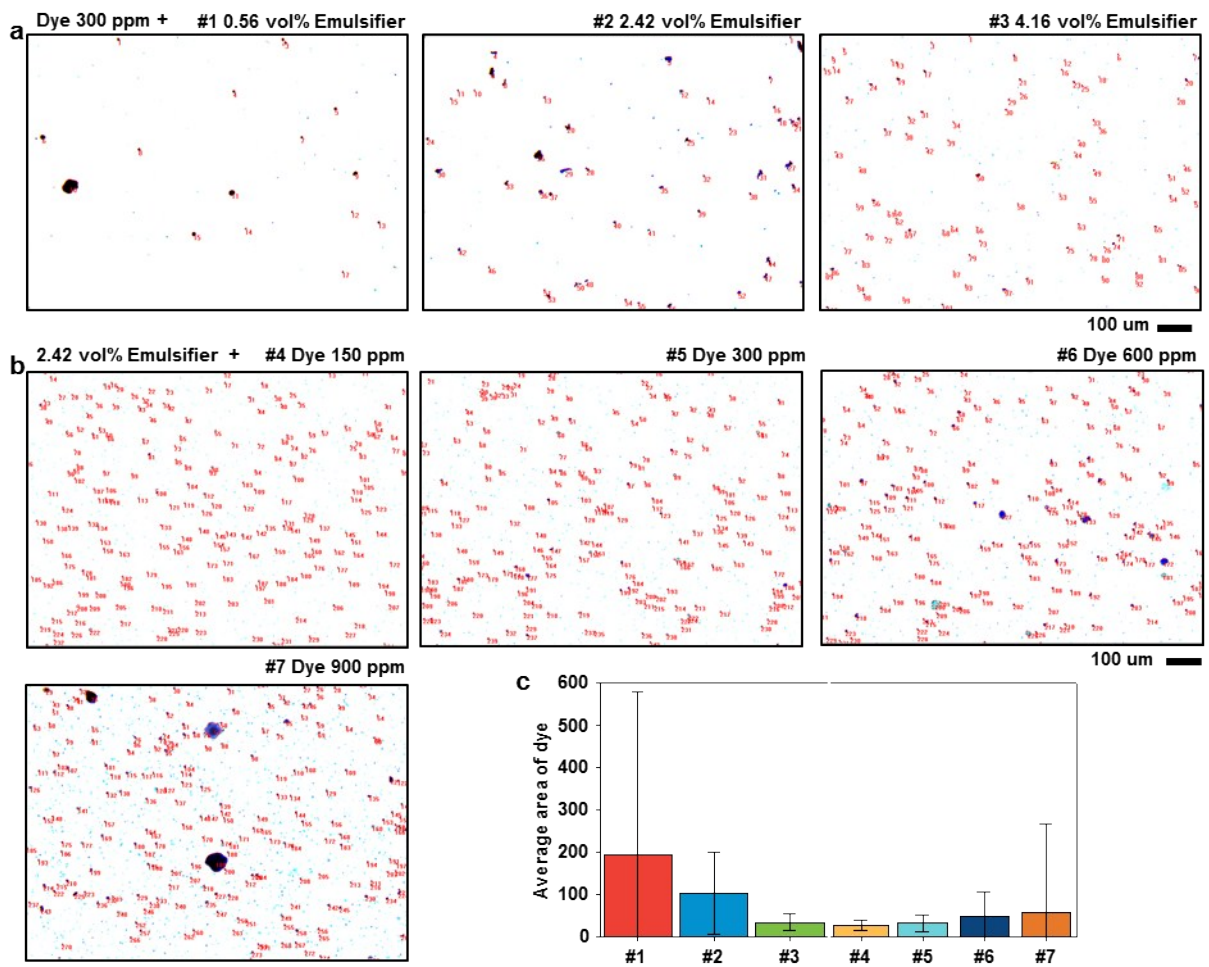


Fig. S4. Comparison of the dispersion shape of the dye by increasing volume of the emulsifier and dye. Image analysis result from Image Pro. (a) the RMI film made with 0.56, 2.42, and 4.16 vol% emulsifier and 300 ppm of dye. (b) The RMI film made with 150, 300, 600 and 900 ppm of dye and 2.42 vol% emulsifier. (c) The average area of dye and standard deviation.

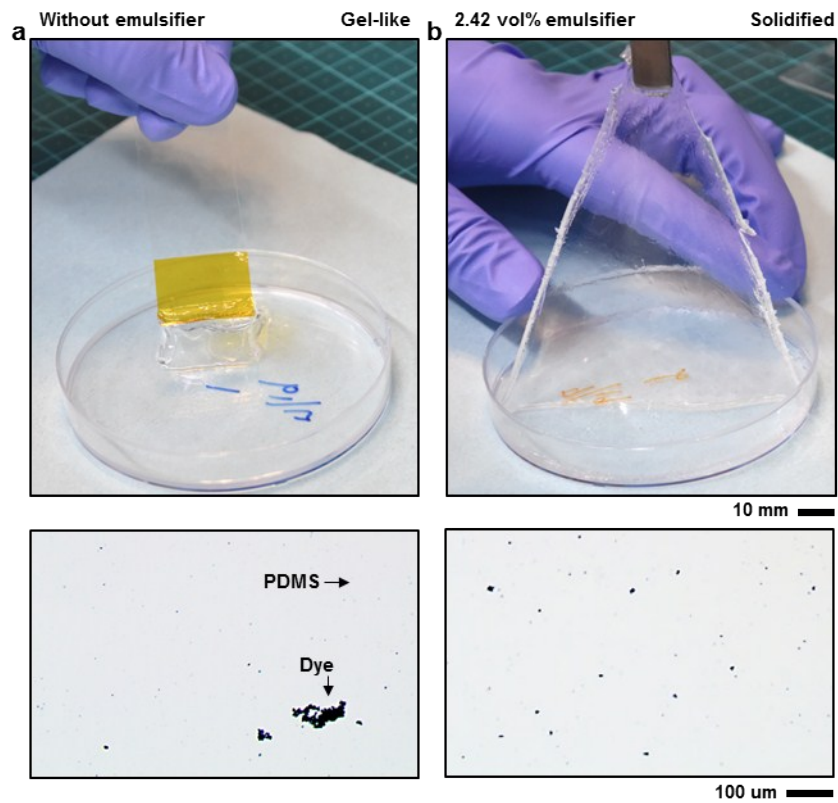


Fig. S5. Effect of emulsifier. Optical images of the RMI film made with (a) 0 and (b) 2.42 vol% emulsifier and 300 ppm of inhibitor. Bottom insets show optical microscopy images of the RMI film made with (a) 0 and (b) 2.42 vol% emulsifier, and 300 ppm of dye.

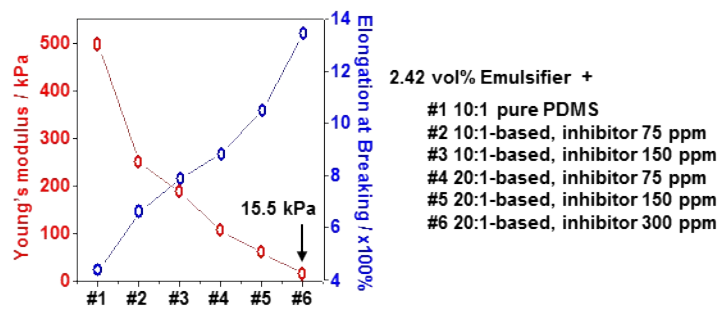


Fig. S6. Chart for the stretchability comparison of the RMI films.

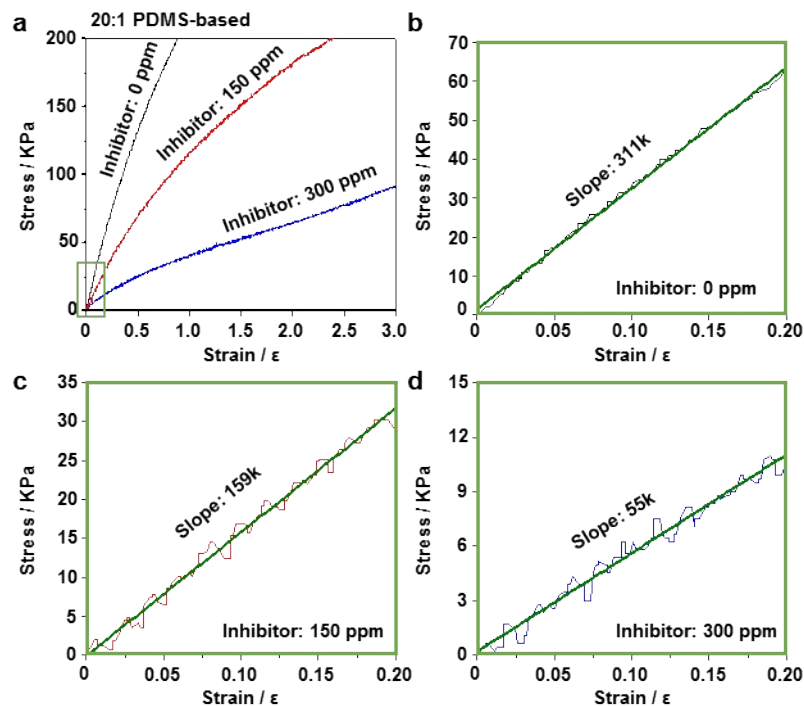


Fig. S7. Young's modulus measurement. (a) Stress–strain curves of RMI films fabricated with 20:1 PDMS and different amounts of the inhibitor. (b-d) Magnified stress-strain curve. The stress-strain curves have an elastic zone up to 0.20 strain.

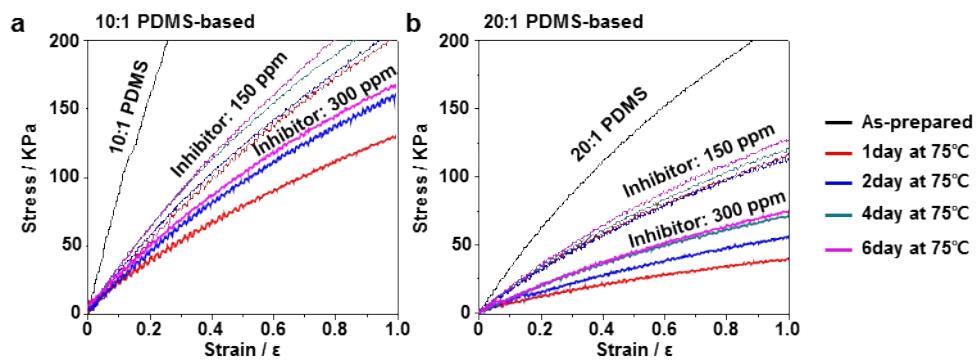


Fig. S8. The effect of long-term storage. (a) Stress–strain curves of RMI films fabricated with 10:1 PDMS and different amounts of the inhibitor. (b) Stress–strain curves of RMI films fabricated 20:1 PDMS and different amounts of the inhibitor. Young’s modulus of 10:1 PDMS-based 150 ppm film changed from 272 kPa to 312 kPa while 300 ppm film changed from 163 kPa to 222 kPa. And Young’s modulus of 20:1 PDMS-based 150 ppm film changed from 159 kPa to 174 kPa while 300 ppm film changed from 55 kPa to 98 kPa.

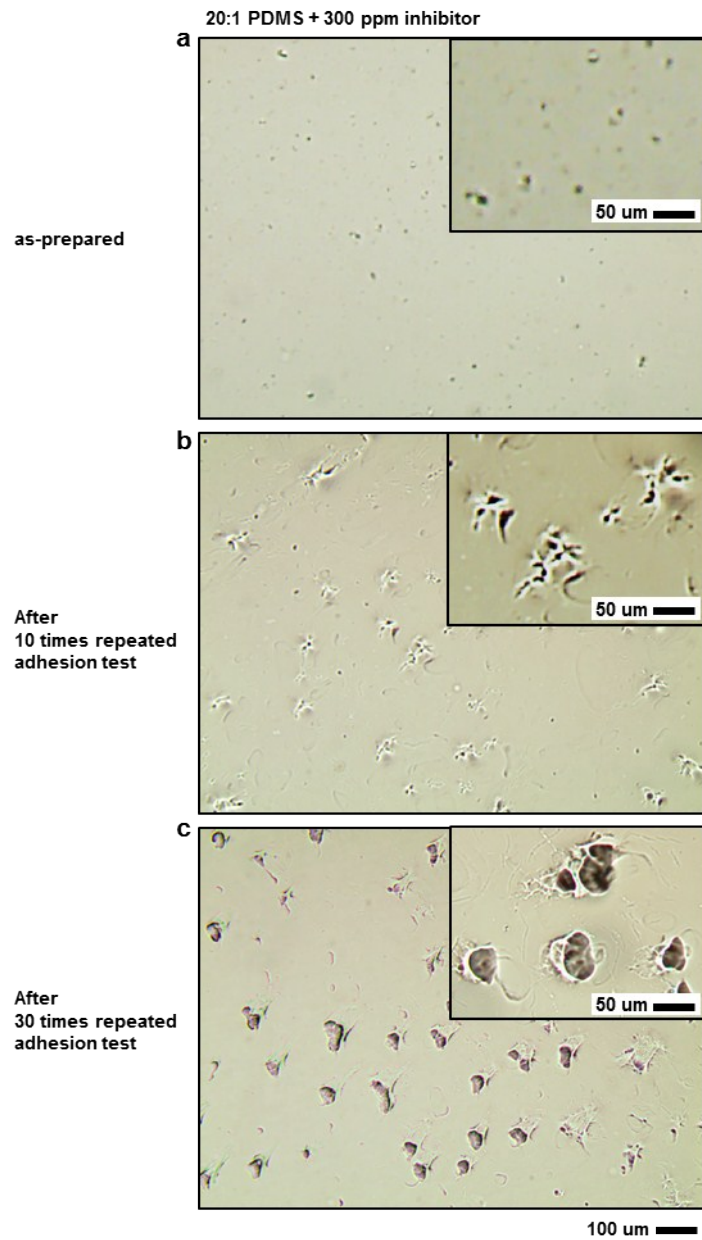


Fig. S9. (a-c) Observing a 20:1 PDMS-based 300 ppm film with an optical microscope after 0-, 10-, 30-cycle adhesion test. The inner elastomer is exposed to the surface by repeated adhesion test, and thereby, the adhesion force of RMI film was recovered.

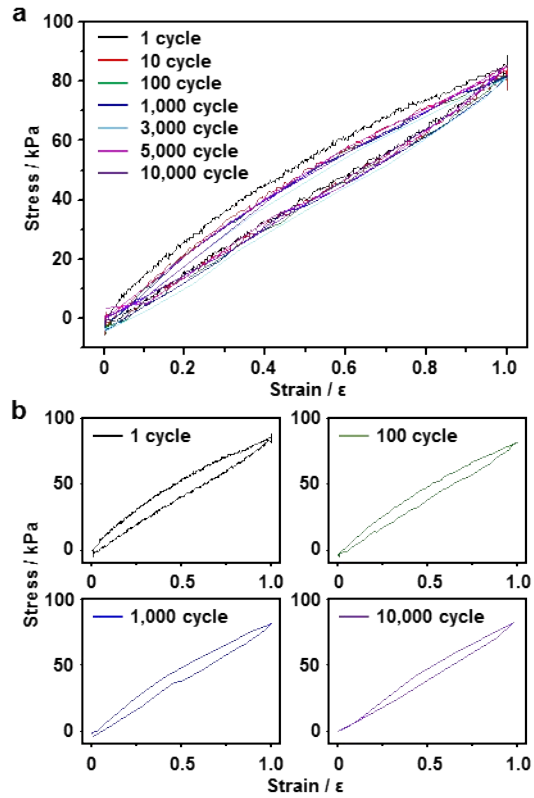


Fig. S10. Hysteresis loop of the RMI film. (a) The cyclic strain-stress curves of the RMI film made with 300 ppm of inhibitor and 20:1 PDMS. (b) Enlarged view of the hysteresis loop for cycle number 1, 100, 1,000, and 10,000. Even increasingly larger cycle number, the hysteresis loop has not shifted.

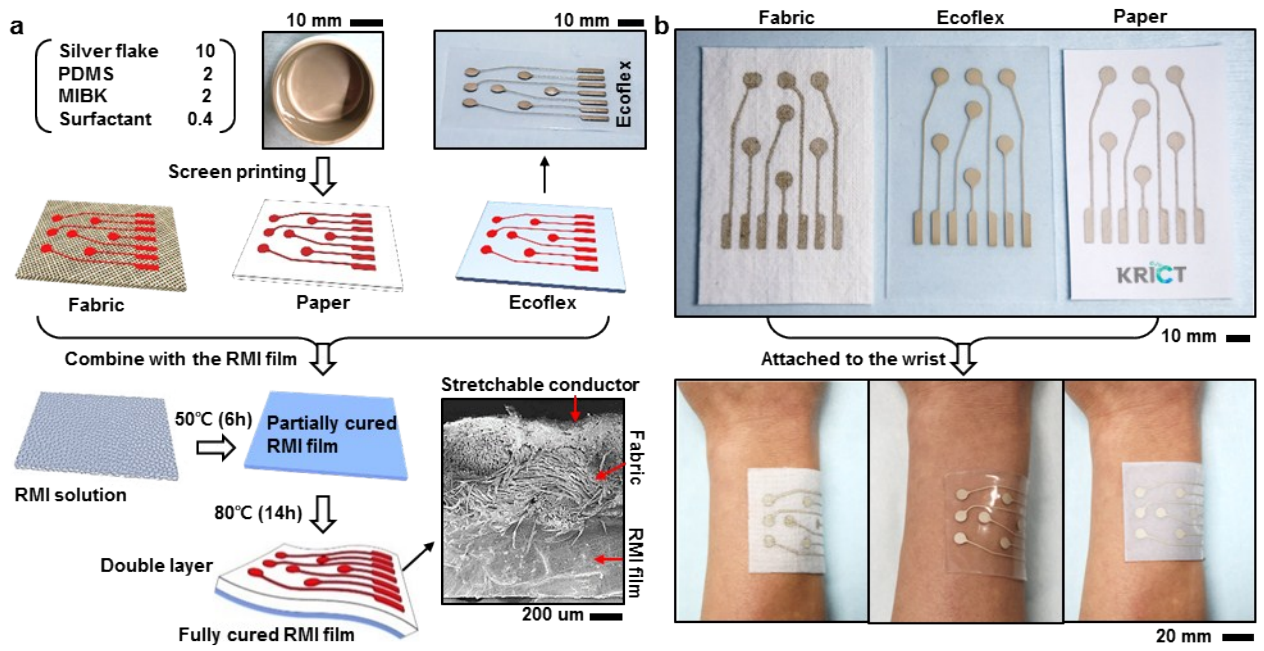


Fig. S11. Functionalization method for the RMI film. (a) Detailed flowchart showing the fabrication process of the double-layer film. For a capacitance sensitivity, the silver paste printed on the fabric, Ecoflex, and paper films. Then, these were combined with the RMI film to form a double-layer and attached to the wrist. (b) Corresponding photograph images.

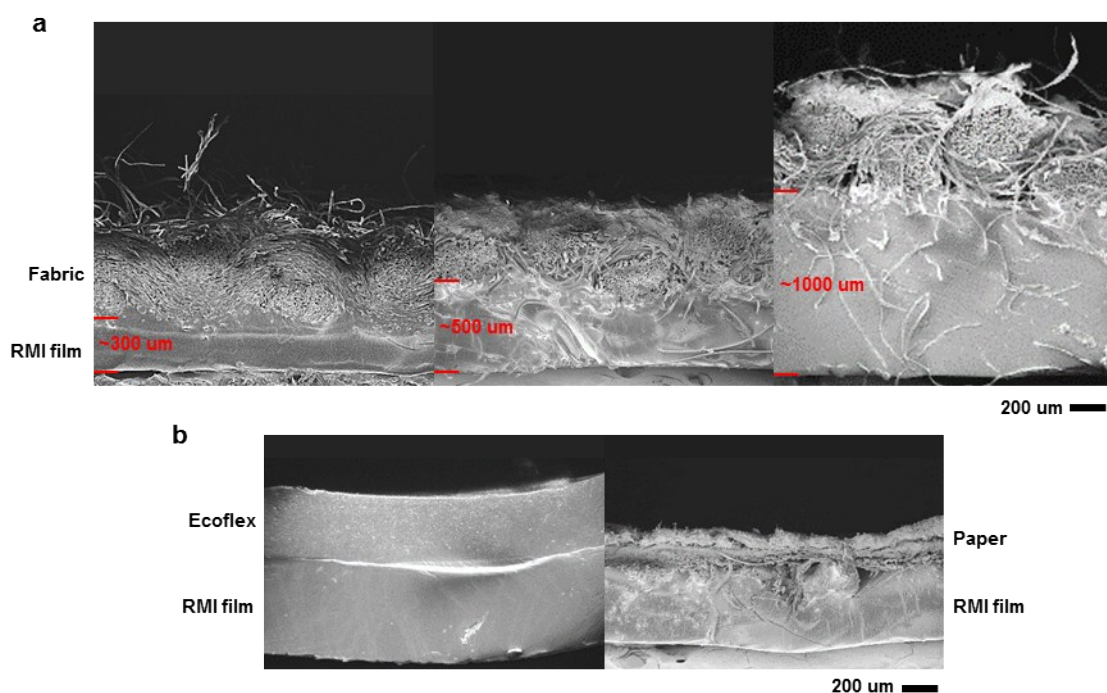


Fig. S12. Thickness comparison of the RMI film. (a) SEM images of the double layer film with 300 μm (left), 500 μm (mid), and 1000 μm (right) of the RMI film. (b) SEM images of the double layer film with the active layer made of Ecoflex (left) and paper (right).

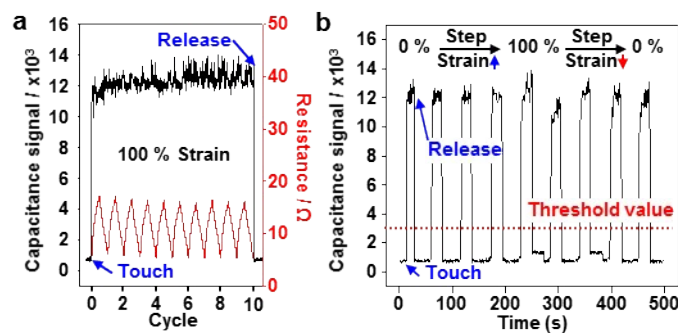


Fig. S13. Resistance and capacitance analysis. Cyclic stretching tests of a capacitance sensor on an Ecoflex film. The analyses were conducted during (a) 100% stretching 10 times and (b) step cyclic stretching test. For the capacitance test, the sensor was touched and released by a finger during the analysis.

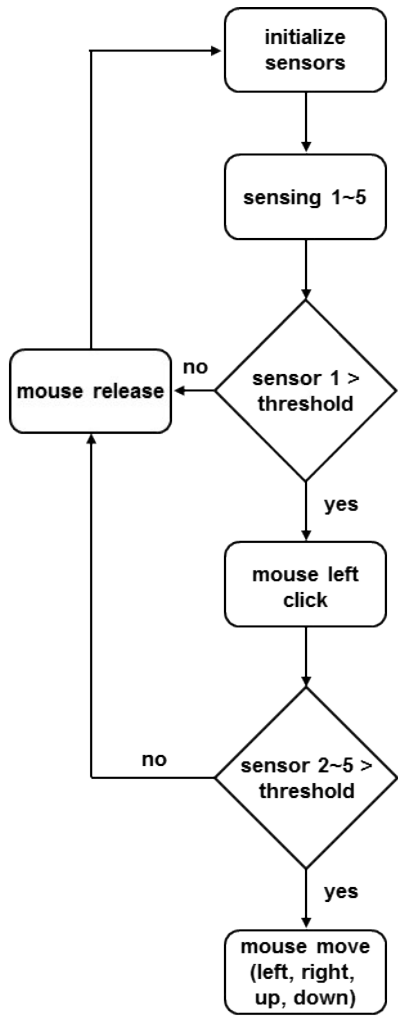


Fig. S14. Process flow chart of the mouse control.

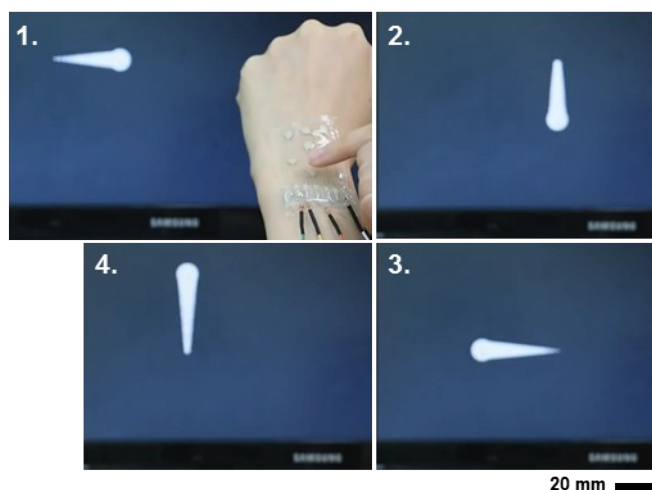


Fig. S15. Sequential photographs of the mouse movement. Snap shots of the mouse movements during square drawing.

Supplementary Table

Inhibitor	300 ppm	430 ppm
10:1 PDMS-based	0.344 N cm ⁻¹	0.416 N cm ⁻¹
20:1 PDMS-based	0.452 N cm ⁻¹	0.736 N cm ⁻¹

* ASTM D3330, @ SUS304 surface

Table S1. 90-degree angle peel test result on SUS304.

10:1 PDMS-based

Amount of inhibitor	Tear-resistance (kN/m)
0 ppm	2.6
75 ppm	4.3
150 ppm	2.7
300 ppm	2.1

* ASTM D624, @ KOPTRI

Table S2. Tear-resistance test results. Test speed was 500 mm/min and the gap between the grips was 65 mm.